Cell Volume Kinetics of Adherent Epithelial Cells Measured by Laser Scanning Reflection Microscopy: Determination of Water Permeability Changes of Renal Principal Cells

Kenan Maric,* Burkhard Wiesner,* Dorothea Lorenz,* Enno Klussmann,* Thomas Betz,† and Walter Rosenthal*‡

*Forschungsinstitut für Molekulare Pharmakologie, D-10315 Berlin, †Carl Zeiss, Mikroskopie, Vertrieb Berlin, D-10787 Berlin, and ‡Freie Universität Berlin, Institut für Pharmakologie, D-14195 Berlin, Germany

ABSTRACT The water channel aquaporin-2 (AQP2), a key component of the antidiuretic machinery in the kidney, is rapidly regulated by the antidiuretic hormone vasopressin. The hormone exerts its action by inducing a translocation of AQP2 from intracellular vesicles to the cell membrane. This step requires the elevation of intracellular cyclic AMP. We describe here a new method, laser scanning reflection microscopy (LSRM), suitable for determining cellular osmotic water permeability coefficient changes in primary cultured inner medullary collecting duct (IMCD) cells. The recording of vertical-reflection-mode *x-z*-scan section areas of unstained, living IMCD cells proved useful and valid for the investigation of osmotic water permeability changes. The time-dependent increases of reflection-mode *x-z*-scan section areas of swelling cells were fitted to a single-exponential equation. The analysis of the time constants of these processes indicates a twofold increase in osmotic water permeability of IMCD cells after treatment of the cells both with forskolin, a cyclic AMP-elevating agent, and with *Clostridium difficile* toxin B, an inhibitor of Rho proteins that leads to depolymerization of F-actin-containing stress fibers. This indicates that both agents lead to the functional insertion of AQP2 into the cell membrane. Thus, we have established a new functional assay for the study of the regulation of the water permeability at the cellular level.

INTRODUCTION

Water permeability across biological membranes has been extensively investigated. Because pure lipid bilayer membranes are weakly permeable to water, pore-like structures facilitating the water transport across bilayered biological membranes were postulated first in the 1950s (Koeford-Johnson and Ussing, 1953). The first proof for a protein acting as a membrane spanning water-selective pore was provided by Preston et al. (1992), using *Xenopus* oocytes microinjected with mRNA encoding aquaporin-1, originally named CHIP-28.

In contrast to electrophysiological measurements of ion currents, which allow high time and signal resolution at the level of a single cell and even a single channel, the techniques available for the measurement of water transport across cell membranes are restricted due to the uncharged nature of water molecules. For example, the determination of water flow across artificial membranes or intact epithelia such as freshly isolated single nephron fragments in microperfusion experiments (Burg et al., 1966) had to be performed using tritiated water. At the single-cell level, the measurement of water permeabilites was performed by monitoring an indirect parameter, the cell volume, determined after three-dimensional reconstruction of the cell shape (e. g. Fisher et al., 1981). Although this method afforded accurate cell volume determination it was relatively slow. To improve the time resolution, approaches to determine water transport across cell membranes of adherent single cells using two types of markers were introduced. In the first approach, fluorescent microbeads were fixed with gelatin on the culture dishes before seeding of epithelial cells and again applied before the experiment to the apical membranes of the cells grown in the pretreated culture dishes. The change in the distance separating the apically localized beads from those on the dishes served as a one-dimensional measure of cell volume changes after an osmotic challenge (Crowe and Wills, 1991). This technique was improved by van Driessche et al. (1993) using an automatically focusing bead-tracking device driven by a piezoelectric motor to move a microscope objective. Second, to measure changes in cell volume, the fluorescent dye calcein-AM was entrapped within the cells and analyzed by total internal reflection microflourimetry. An increase in cell volume results in a decreased fluorescence signal from the cytosol, whereas increasing fluorescence intensity indicates cell shrinkage (Farinas et al., 1995). Recently a new technique, scanning ion conductance microscopy (Korchev et al., 2000), has been described, which allows high time resolution (milliseconds) for measurement of cell height changes but requires the addition of piezo stepper-driven equipment and microelectrode amplifiers to the microscope. In this study, a comparison of cell height measurement by scanning ion conductance microscopy with the determination of cell volume changes by preloaded fluorophores showed comparable results.

We present a novel optical method to continuously monitor cell volume changes using a confocal laser scanning

Received for publication 9 August 2000 and in final form 2 January 2001.

Address reprint requests to Dr. Kenan Maric, Forschungsinstitut für Molekulare Pharmakologie, Robert-Roessle-Strasse 10, 13125 Berlin, Germany. Tel.: 49-030-94793-260; Fax.: 49-030-94793-109; E-mail: maric@fmp-berlin.de.

0006-3495/01/04/1783/08 $2.00

microscope. Instead of using preloaded cellular indicators, we applied the so-called reflection mode of confocal laser scanning microscopy to visualize vertical sections of unstained, living cells. Because of the different optical densities of the coverslip glass, the intracellular fluids and the bilayered cell membrane, the laser beams are reflected at these optical borders and return through the objective to the photomultiplier as in fluorescence microscopy (see Fig. 1). Thus, the movement of the plasma membranes of swelling or shrinking cells can be tracked directly by reflected laser beams. The parameter used to determine the kinetics of swelling or shrinking cells by laser scanning reflection microscopy (LSRM) is a two-dimensional optical vertical section through the cells. It is noteworthy to mention that LSRM is different from the reflection interference contrast microscopy (e.g., Filler and Peuker, 2000), which uses optical phenomena caused by oblique epi-illumination from a monochromatic light source.

Primary cultured inner medullary collecting duct (IMCD) cells are a cellular model consisting mainly of vasopressin-sensitive principal cells responsible for water reabsorption within the collecting duct. Cultured IMCD cells endogenously express the vasopressin-regulated antidiuretic machinery, in particular the vasopressin V2 receptor and the water channel aquaporin-2 (AQP2) (Maric et al., 1998). Incubation of IMCD cells with cAMP-elevating agents (arginine-vasopressin or forskolin) induces the translocation of AQP2 to the cell membrane, similar to principal cells in vivo. In addition, incubation of the cells with *Clostridium difficile* toxin B, which leads to depolymerization of F-actin-containing stress fibers by inhibiting members of Rho-family proteins (Hall, 1998; Lerm et al., 2000), has been shown to induce hormone independently the translocation of AQP2 to the cell membrane (Klussmann et al., 2001). The hormone-induced trafficking of AQP2 was described as the shuttle hypothesis (Wade et al., 1981).

We have applied LSRM to study the effects of forskolin and toxin B on the regulation of osmotic water permeability in IMCD cells. Osmotic water permeability changes could be induced by the cAMP-elevating agent forskolin and hormone independently by toxin B. The specificity of the effect of *C. difficile* toxin B on primary cultured IMCD cells was verified by application of the toxin on Madin-Darby canine kidney (MDCK) cells, which are void of the above mentioned proteins of the antidiuretic machinery.

MATERIALS AND METHODS

Cell culture

IMCD cells were prepared and cultured as described (Maric et al., 1998). Briefly, Wistar rats were killed by decapitation, and kidney inner medullae (including papillae) were removed and cut into small pieces. Tissue was digested in phosphate-buffered saline (PBS: 137 mM NaCl, 2.7 mM KCl, 1 mM KH_2PO_4, 10 mM Na_2HPO_4, pH 7.4) containing 0.2% hyaluronidase (Boehringer Mannheim, Mannheim, Germany) and 0.2% collagenase type CLS-II (Biochrom, Berlin, Germany) at 37°C for 90 min. Thereafter cells were centrifuged (5 min; 300 × *g*), washed three times, and seeded at a density of approximately 7×10^4 cells/cm^2 on glass coverslips (30 mm diameter) coated with type IV collagen (2 μg/cm^2; Becton-Dickinson, Heidelberg, Germany) in petri dishes. Because IMCD cells are accustomed to high osmotic challenges within the kidney medulla, Dulbecco's modified Eagle's medium (DMEM), adjusted to 600 mOsm/kg by addition of 100 mM NaCl and 100 mM urea, was used to establish growth conditions with preferential selectivity for IMCD principal and intercalated cells (Mooren and Kinne, 1994). Penicillin (100 IU/ml), streptomycin (100 μg/ml), glutamine (2 mM), nonessential amino acids (1%), fetal calf serum (10%), and dibutyryl cyclic AMP (DBcAMP; 500 μM) were routinely added. The cell culture medium was exchanged three times per week. Approximately 18 h before the experiments, the medium was replaced by cell culture medium without DBcAMP to render the cells readily stimulable by cAMP-elevating agents.

MDCK cells (strain II) were kept in DMEM (osmolality of 300 mOsm/kg) containing penicillin (100 IU/ml), streptomycin (100 μg/ml), and fetal calf serum (10%). MDCK cells were used from passage 48 to passage 52.

Fluorescence microscopy and visualization of F-actin

For fluorescence microscopy cells were grown on glass coverslips (12 mm diameter) as described above. IMCD and MDCK cells were left untreated or treated with *C. difficile* toxin B in different concentrations (4 μg/ml to 4 ng/ml) to estimate appropriate concentrations of the toxin for both cell types (i.e., depolymerization of stress fibers). For visualization of the F-actin-containing stress fibers, both cell types were fixed and permeabilized as described (Maric et al. 1998). They were incubated with phalloidin-TRITC (100 μg/ml) for 30 min and subsequently washed with PBS. Fluorescence signals were analyzed by epifluorescence microscopy (Leica DMLB microscope with cooled Sensicam 12 bit CCD camera, Bensheim, Germany).

Measurements of cell volume kinetics by LSRM *x-z*-scan time series

Bathing solutions

The above described cell culture media were used as experimental bathing solutions with two exceptions: 1) instead of the bicarbonate/CO_2-based buffer system, HEPES-buffer (10 mM) served to maintain a constant pH of 7.4 under room air conditions, and 2) fetal calf serum was replaced by sorbitol to adjust the osmolality to 600 mOsm/kg for IMCD cells and to 300 mOsm/kg for MDCK cells. These normotonic (N) bathing solutions were diluted with distilled water to obtain hypotonic (H) solutions.

For validation experiments on IMCD cells (see Results), solutions with osmolalities from 100 up to 900 mOsm/kg were used. The solutions with higher osmolalities (750 mOsm/kg) were obtained by further addition of NaCl and urea (50 mM each) and solutions with an osmolality of 900 mOsm/kg by addition of 100 mM of each of these compounds.

For functional experiments determining P_f changes, only N and H solutions with osmolalities of 600 and 200 mOsm/kg, respectively, were used for IMCD cells, whereas MDCK cells were bathed in N and H solutions with osmolalities of 300 and 100 mOsm/kg, respectively. The osmotic challenge for both cell types was therefore considered to be identical (threefold dilution of the appropriate solution osmolalities).

Preparation of cells for cell volume kinetics measurements

In primary cultured IMCD cells, the vasopressin-regulated water channel AQP2 is sorted mainly to the lateral (rather than the apical) membranes

upon stimulation with forskolin or vasopressin (Maric et al., 1998; Klussmann et al., 1999, 2000). To ensure free access of bathing solutions to the lateral membranes, IMCD cells were artificially made noncoherent by trypsinization (37°C; 8 to 12 min with 0.05% trypsin/0.02% EDTA; Biochrom). After being allowed to recover from the trypsinization procedure for at least 2 h under growth conditions, the IMCD cells were washed twice with bathing solution N (600 mOsm/kg). The coverslip with the cell layer was carefully removed from the culture dish and mounted for the entire experiment in a custom-made cuvette fitted into the motor-driven *x-y* table of the laser scanning microscope (LSM 410, Zeiss, Jena, Germany).

MDCK cells were cultured until they reached a subconfluent density, washed twice with the appropriate bathing solution N (300 mOsm/kg), and mounted as described for IMCD cells.

Cell swelling reaction and data acquisition

Appropriate cells, i.e., individualized cells that morphologically resembled principal cells and to whose lateral membranes solute had free access, were selected using the transmission mode of the LSM 410 (Fig. 1). Next, the optical setting of the LSM 410 was changed to the reflection mode using a long-pass emission filter of 515 nm, thus allowing the recording of the reflected laser beam with 543 nm wavelength (Fig. 1). In contrast, an appropriate setting for fluorescence microscopy would use a long-pass emission filter of 570 nm to allow for the recording of the light emitted by a fluorophore (e.g., TRITC; $\lambda = 582$ nm) that is excited by the laser with a wavelength of $\lambda = 543$ nm (Fig. 1). Cells were scanned with a ×63 magnification water immersion objective, numerical aperture 1.2. The initially applied bathing solution N (600 mOsm/kg for IMCD cells and 300 mOsm/kg for MDCK cells) was removed by suction using a peristaltic pump, leaving only a very thin film of solution (~20 μm) above the cells. Cell swelling was then initiated by the application of bathing solution H (200 mOsm/kg for IMCD cells and 100 mOsm/kg for MDCK cells). Customized macro-programming facilitated the recording of reflection-mode *x-z*-scans with a frequency of 0.25 Hz; *x-z*-scans were stored as time series. All recordings were started 40 s before the change of N to H bathing solution and continued for 200 s. The osmotic challenges were performed and monitored on the microscope at elevated room temperature (27°C). Thereafter, cells were allowed to recover from the osmotic challenge in bathing solution N. For this purpose they were placed inside the metal cuvette on a precision heating block (33°C; Precitherm, Duesseldorf, Germany) under occlusion to prevent evaporation and thus uncontrolled increase of the osmolality of the bathing solution. During this period (up to 3 h 30 min), cells were either left untreated or stimulated as indicated in the Results. Recovery or incubation of the cells at temperatures higher than 33°C led to a displacement of the cells within this period, whereas at lower temperatures no effects of the toxin or forskolin were observed. Following exchange of bathing solutions from N to H, swelling of the same cells was recorded for a second time (27°C) as described above. Cells were located by adjusting the coordinates of the motor driven *x-y* table of the microscope to the previously recorded position. This procedure was validated before with fixed and stained cells.

Data analysis

To determine the increase of vertical *x-z*-scan section areas from single cells, the *x-z*-scan time series were processed using the KS 400 image analyzing software (Carl Zeiss Vision, Hallbergmoos, Germany). A macro-programmed analysis sequence was used, which is schematically shown in Fig. 2. Initially, a single cell was chosen by defining a rectangular region of interest. The subsequent processing included digital smoothing followed

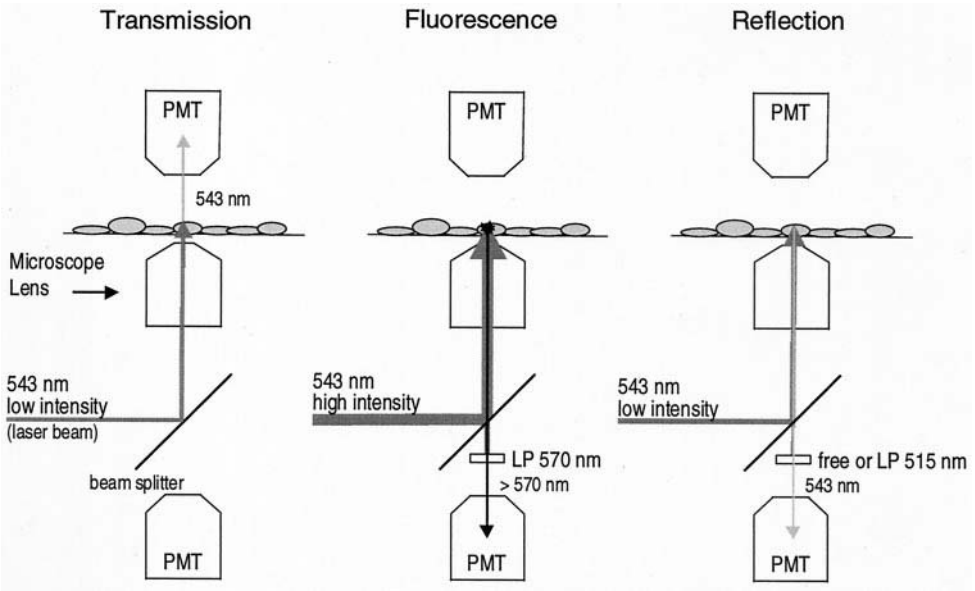

FIGURE 1 Visualization modes for cell monolayers using the laser scanning microscope. The schematic drawing illustrates three major possibilities to visualize monolayers of cells. 1) Transmission: conventional microscopy does not necessarily require a laser scanning apparatus. Without additional contrasting devices (phase-contrast, differential interference contrast) or staining of the cells, no satisfactory results are achievable. Cells can be visualized only in the plane of the coverslip by the photomultiplier (PMT). 2) Fluorescence microscopy monitors the light emitted by excited fluorophores back through the objective to the PMT. Fluorophores have to be introduced into the cells before the experiment. An optical long-pass emission filter (LP570) serves to separate the light emitted by fluorophores ($\lambda > 570$ nm) and the inevitably reflected light (excitation wavelength for fluorescence; $\lambda = 543$ nm). Vertical optical sectioning (*x-z*-sections) of the cells is enabled by the scanning apparatus. 3) Reflection microscopy records the light reflected at the borders of media of different optical density (intra- and extracellular lumen; cell membranes). As in the fluorescence mode, the laser scanning apparatus allows the recording of vertical *x-z*-sections. In contrast to fluorescence microscopy, however, no filtering of the emitted light is required. In the case of the LSM 410, we used the integrated HeNe laser emitting green light at 543 nm and a long-pass emission filter at 515 nm (LP515).

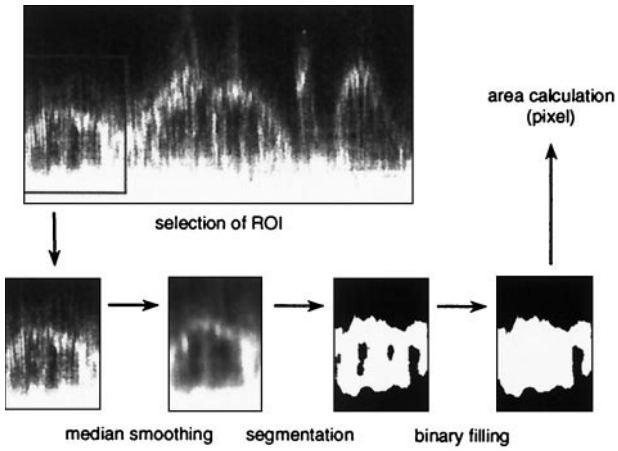

FIGURE 2 Interactive area determination of reflection-mode *x-z*-scans. Schematic illustration of the macro-programmed analysis sequence leading to the determination of longitudinal *x-z*-scan section areas *a*. For detailed description see Materials and Methods.

by an interactive segmentation of the chosen region to yield a maximally contrasted cell contour, which was thereafter filled with pixels. The number of pixels served as a measure of the vertical *x-z*-scan section area (a) of a cell. This process was repeated for the entire time series, giving a raw data table of the longitudinal *z*-section area increase as a function of time, $a(t)$, for each analyzed single cell.

Calculation of permeability coefficient changes

The osmotic water permeability coefficient P_f can be calculated for single adherent cells by Eq. 1 in a simplified approach explained in detail by Farinas et al. (1995):

$$P_f = (\tau(A/V)_o V_w \phi_o)^{-1}, \quad (1)$$

where τ represents the time constant of the exponential function describing cell volume changes due to osmotic challenges, $(A/V)_o$ is the ratio of cell surface area A to volume V before the swelling reaction, ϕ_o is the initial osmolality of the bathing solution, and V_w is the molar volume of water (18 cm^3/mol).

The time constant τ of the swelling process was obtained by fitting Eq. 2 to the experimentally obtained vertical *x-z*-scan section areas a after the osmotic challenge, assuming that cell shape changes occur only in the vertical direction (see Results for validation of vertical *x-z*-scan section areas as a measure for cell volume):

$$a(t) = a_{min} + (a_{max} - a_{min})(1 - e^{(-t/\tau)}) \quad (2)$$

Fitting was performed by nonlinear regression analysis, using the Levenberg-Marquardt method within the GraphPad Prism software for Windows (version 3.00, GraphPad Software, San Diego, CA). Values of τ determined by the fitting process of the exponential function $a(t)$ to the raw data of a were included for further analysis only when the correlation coefficients R^2 for the fitted to the raw data of $a(t)$ were ≥ 0.90. An example of the obtained fits to raw data of a swelling IMCD cell before and after stimulation with forskolin is shown in Fig. 3.

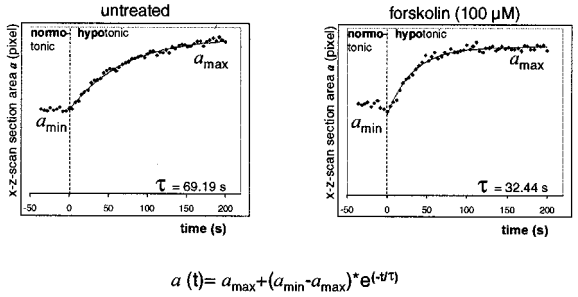

FIGURE 3 Determination of the time constants of cell swelling. Raw data of vertical *x-z*-scan section areas a were fitted to the shown exponential function (Eq. 2) for determination of the time constants τ of the swelling processes before (*left*) and after (*right*) stimulation of cells with forskolin (100 μM; 30 min). Forskolin reduced the time constant τ by ~50%, indicating a twofold acceleration of the swelling process.

RESULTS

LSRM and validation of the vertical *x-z*-scan section area *a* as a measure for cell volume changes

Fig. 4 shows typical LSRM *x-z*-scans of IMCD cells under normotonic conditions and 8 and 80 s after a challenge with hypotonic bathing solution, respectively. Although neither fixed nor stained, the cell shapes are visualized by reflected light in these optical sections. The figure illustrates that swelling of the cells results in an increase in cell height, whereas lateral movements are not evident, as indicated by the unchanged distance between the cells during the swelling process (bar, 110 μm in all panels). This finding led to the assumption that the vertical *x-z*-scan section area of each cell might serve as an appropriate parameter to monitor cell volume changes in response to osmotic challenges. To confirm this, experiments were performed to measure the correlation between vertical *x-z*-scan section areas a and the osmolalities of the bathing solutions. IMCD cells adapted to the cell growth media (600 mOsm/kg) were challenged with bathing solutions with osmolalities ranging from 100 to 900 mOsm/kg. After an equilibration period of 5 min for each osmolality, *x-z*-scans were recorded, and vertical *x-z*-scan section areas a were subsequently determined for each cell ($n = 5$), as described in Materials and Methods and in Fig. 2. The *x-z*-scan section areas a (in percentage of normotonic cells) were then plotted as a function of bathing solution osmolality ϕ (Fig. 5), which could be fitted to a hyperbolic function for $a(\phi)$, given below in Eq. 6.

As described in Farinas et al. (1995), cell volume V is related to solution osmolality ϕ by the relationship

$$(V - b)/(V_o - b) = \phi_o/\phi, \quad (3)$$

where the parameter b represents osmotically inactive parts of the cell volume and therefore has to be subtracted from total cell volume V. If Δx represents the thickness of the vertical *x-z*-scan section area a and s is the vertical section

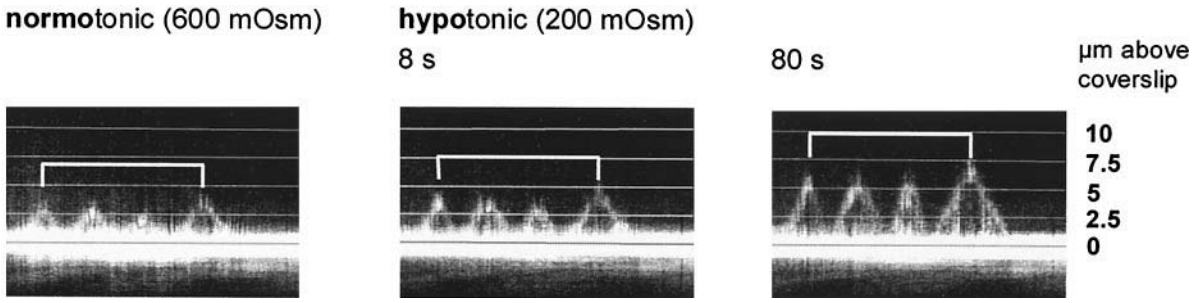

FIGURE 4 Cell volume kinetics of primary cultured principal cells measured by LSRM. Vertical reflection-mode *x-z*-scans of unstained, living IMCD cells are shown in normotonic bathing solution and at 8 and 80 s after application of hypotonic bathing solution (see Material and Methods). Four single cells are visualized. Hypotonicity-induced cell swelling can be monitored by the increase in cell height. The strong reflection signal at the cell base represents the border of the coverslip. Apical cell membranes are visualized by a less intense reflection signal (×63 magnification, water immersion lens; nonproportional image with a ratio of 1:4 for *x*:*z*). The bar (110 μm in all panels) indicates that cell swelling does not influence cell width.

area of osmotically inactive parts assuming the osmolality to be homogenous within ($V - b$), then the replacement of the three-dimensional variables V and b by the products of vertical areas a with Δx and of s with Δx within Eq. 3 results in

$$(a - s)\Delta x/(a_o - s)\Delta x = \phi_o/\phi, \quad (4)$$

which can be solved for a and written as a function of ϕ,

$$a(\phi) = s + (a_o - s)\phi_o/\phi \quad (5)$$

by replacing $(a_o - s)\phi_o$ with the factor c, in the relationship

$$a(\phi) = s + c/\phi. \quad (6)$$

The parameter c represents a proportionality factor for the relationship of $(a - s)$ to ϕ. Therefore, under the given assumptions, the cell swelling/shrinking process and thus cell volume changes in response to osmotic challenges can be delineated from changes of the vertical *x-z*-scan section areas a given in Eq. 6. In fact, Eq. 6 could be well fitted to the experimentally obtained *x-z*-scan section areas a of IMCD cells for different osmolalities (Fig. 5) with $R^2 > 0.96$ ($s = 64.81$; $c = 22290$). This allows the conclusion that the vertical *x-z*-scan section area a serves as a valid parameter to monitor cell volume changes in response to osmolality changes.

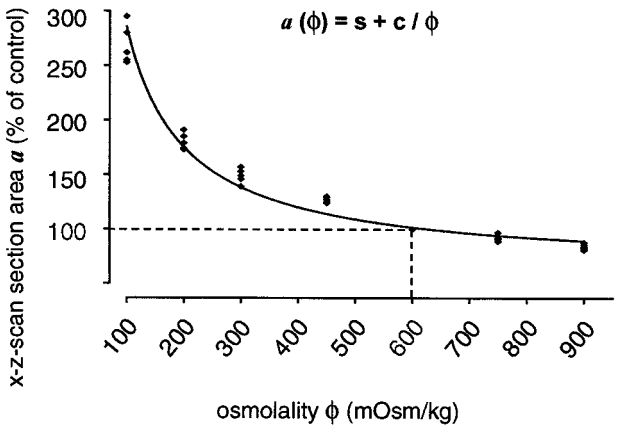

FIGURE 5 Correlation of *x-z*-scan section changes with bathing solution osmolalities. The dashed lines indicate the control conditions for cultivation of IMCD cells (DMEM adjusted by NaCl and urea to 600 mOsm/kg, i.e., normotonic bathing solution). Cells ($n = 5$) were challenged with bathing solutions of the indicated osmolalities and *x-z*-scan section areas a are given in percentage of control cells. The fit of the raw data points results in a hyperbolic correlation ($R^2 > 0.96$; $s = 64.81$; $c = 22290$). The swelling and shrinking behavior of IMCD cells as measured by vertical *x-z*-scan sections therefore resembles that of an osmometer.

Functional experiments determining osmotic permeability changes

A coverslip with subconfluent IMCD or MDCK cells (see Materials and Methods) was mounted in a cuvette and transferred to the LSM. LSRM *x-z*-scan sections were recorded, while the cells were challenged osmotically (N to H) by exchanging the bathing solutions. After a second exchange (H to N), the cells were allowed to recover from the osmotic hypotonicity challenge on the heating block (33°C; see Materials and Methods). During this time the IMCD cells were kept under control conditions (i.e., buffer solution) and were treated with the cAMP-elevating agent forskolin (50 μM, 30 min) or with toxin B (4 μg/ml; 3 h 30 min), which irreversibly inactivates small GTPases of the Rho family. MDCK cells, which served as a negative control for the experiments with toxin B, were much more sensitive to the action of toxin B and were therefore incubated with lower concentrations of the toxin (40 ng/ml). The effects of *C. difficile* toxin B on both cell types were assessed before the functional experiments by fluorescence microscopy observing the depolymerization of F-actin by TRITC-phalloidin staining (Fig. 6). After this treatment, hypotonicity-induced cell swelling was again determined using the same cells. The analysis of the recorded time series for the vertical *x-z*-scan section areas a of cells (see Materials and Methods; Fig. 2) before and after the treat-

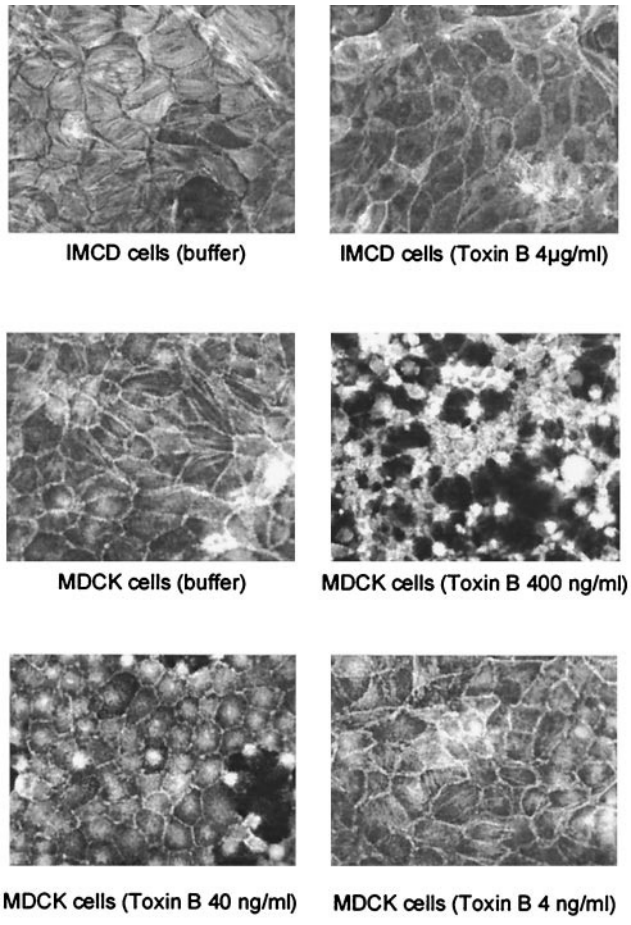

FIGURE 6 The effect *Clostridium difficile* toxin B on the F-actin containing stress fibers in IMCD and MDCK cells. IMCD and MDCK cells were left untreated (buffer) or incubated with *C. difficile* toxin B (4 μg to 4ng/ml for 3 h 30 min). The cells were fixed, permeabilized, and incubated with TRITC-conjugated phalloidin (0.1 mg/ml). Phalloidin staining of F-actin-containing stress fibers was detected by epifluorescence microscopy ($\times$40 magnification).

ment resulted in two exponential swelling curves for each cell. Eq. 2 was then fitted to these raw data curves by nonlinear regression analysis to determine the time constants τ of the swelling process, as shown in Fig. 3.

Investigation of the IMCD cells by transmission and reflection microscopy (not shown) before and after forskolin treatment revealed that the cells did not change their shape. Therefore, identical values for A_o and V_o were used in Eq. 1. The ratio of time constants τ before and after forskolin treatment is inversely related to the ratio of permeability coefficients P_f before and after forskolin treatment. The reduction of time constants thereby indicates a twofold increase of the osmotic water permeability coefficient P_f after forskolin treatment. The results from time constant determinations before and after different treatments are shown and summarized in Fig. 7. The values of the time constants τ before (abscissa) and after (ordinate) treatment, reveal a scattered distribution of data points (each representing data from a single cell) along a regression line, passing through the origin of the coordinate system. By virtue of this arrangement of time constants, the approximate mean change of the water permeability coefficients of the whole population can be delineated from the inverse slope of the linear regression line. As expected, IMCD cells undergoing control treatment (Fig. 7, buffer) show an almost unchanged osmotic water permeability. Forskolin treatment of IMCD cells, however, induced a doubling of osmotic water permeability (Fig. 7, forskolin). The attempt to reverse this acceleration in cell swelling by removal of forskolin from pretreated cells (four washes with excess of forskolin-free bathing solution; 15 min each wash) resulted in a reduction of osmotic water permeability by $\sim$30%, accompanied by a more scattered distribution of data points around the regression line (Fig. 7, forskolin washout). This can be explained by a slow and (between cells) variable removal of forskolin from its intracellular site of action.

The results show that forskolin increases osmotic water permeability presumably by elevating cAMP in IMCD cells. The results are in agreement with the finding that forskolin triggers the translocation of AQP2-bearing vesicles from intracellular domains into the IMCD cell membrane (Maric et al., 1998; Klussmann et al., 1999).

We have recently provided evidence for the involvement of small GTPases of the Rho family in the signal cascade leading to the insertion of AQP2 into the cell membrane (Klussmann et al., 2001). Application of toxin B (4 μg/ml; 3 h 30 min) to IMCD cells (see Materials and Methods) resulted in an acceleration of cell swelling. The inverse slope of the regression line of the time constants τ was 2.55 (Fig. 7, toxin B). As toxin B treatment also induced a shape change of IMCD cells (Klussmann et al., 2001), we included the initial cell surface A_o and the initial cell volume V_o in the analysis, as implied by Eq. 1. Determinations of A_o and V_o were performed by a series of *x*-*y*-reflection-mode sections through entire cells, with a distance of 500 nm between each section (not shown). Cell surface areas A_o were then calculated by summarizing the perimeters of each cell slice, multiplied by the slice thickness, and cell volumes V_o were calculated by summarizing the areas of each cell slice multiplied by the slice thickness of 500 nm. Linear regression analysis of the products of $\tau\ (A/V)_o$ before and after treatment revealed an inverse slope of 2.048 of the resulting regression line, thus indicating that toxin B increases the P_f of IMCD cells to a similar extent as forskolin (Fig. 7, toxin B corrected for $(A/V)_o$). The ratio $(A/V)_o$ ($3144 \pm 346\ cm^{-1}$) inserted into Eq. 1 allowed the calculation of basal osmotic permeability coefficients of IMCD cells ($P_f = 12.76 \pm 3.43\ \mu m/s$; $n = 12$).

To analyze the results of the above experiments statistically, we calculated the quotients of the P_f increases for each individual cell and compared the means of their distributions by nonpaired *t*-tests (Fig. 7, means of individual cells). There were significant differences between control

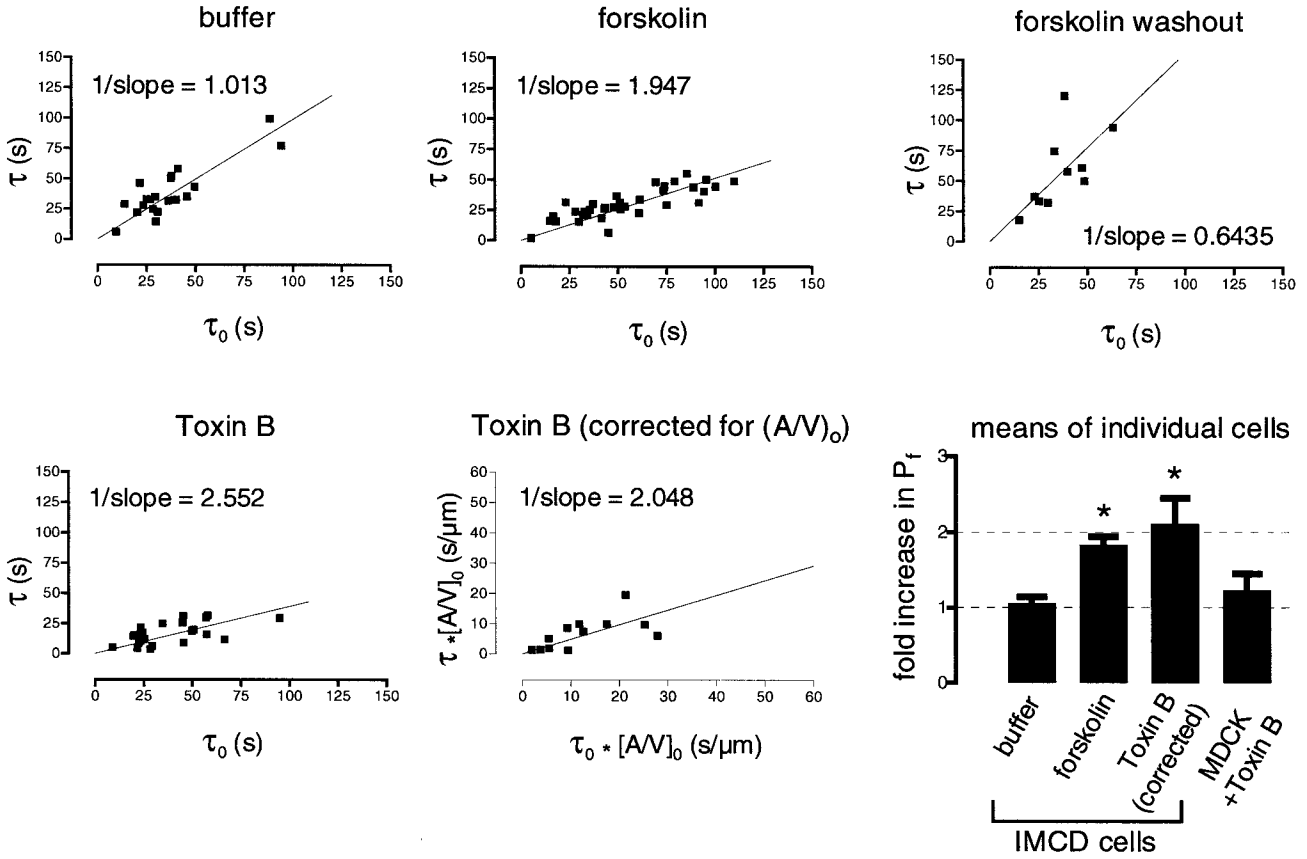

FIGURE 7 P_f changes of IMCD cells depicted as the change of time constants before (τ_o; *abscissa*) and after (τ; *ordinate*) treatment with buffer, forskolin (50 μM; 30 min), or toxin B (4 μg/ml; 3 h 30 min) as indicated. The inverse slopes of the linear regression lines passing through the origin of the coordinate system are given to describe the changes in P_f. Each data point represents one single cell. For statistical analysis, the means of single quotients of the time constants τ determined from IMCD cells and MDCK cells treated with toxin B (40 ng/ml; 3 h 30 min) were analyzed and compared by Student's *t*-test. MDCK cells were used to exclude nonspecific effects of toxin B on IMCD cells' P_f changes. Error bars indicate SEM. Asterisks indicate significant differences from forskolin- and toxin-B-treated IMCD cells from buffer-treated IMCD cells as well as from toxin-B-treated MDCK cells.

(buffer-treated) IMCD cells and IMCD cells treated with forskolin ($p < 0.0001$) and between control and toxin-B-treated cells ($p = 0.0132$). In contrast, the calculated P_f increases for forskolin and toxin-B-treated IMCD cells did not differ significantly from each other ($p = 0.5446$). To exclude the possibility that the observed effect of toxin B might have been nonspecific, we also analyzed data obtained with toxin-B-treated MDCK cells. The mean P_f increase observed in MDCK cells after toxin B treatment (40 ng/ml) was not different from buffer-treated IMCD cells ($p = 0.4794$) but significantly different from forskolin- or toxin-B-treated IMCD cells ($p = 0.0454$ and $p = 0.0223$, respectively). Thus, toxin B increases osmotic water permeability in IMCD cells but not in MDCK cells.

DISCUSSION

We demonstrate here that LSRM is a valid experimental procedure to measure volume changes of adherent cells. As a major advantage of this method, bleaching or quenching effects of fluorophores need not be considered. Other advantages are the acquisition of single-cell kinetic data and the possibility of controlling each cell's swelling behavior by real-time measurements. Cells reacting with excessive, usually irreversible swelling to hypotonic challenge can thus be excluded from further analysis. Laser scanning microscopy is now a broadly established method in cell biology, and the necessary features for the kind of recordings presented here can be relatively easily implemented provided one's instrument is equipped for making true vertical *x*-*z*-scans.

To minimize errors we calculated, instead of absolute P_f values, the changes of P_f before and after stimulation of the cells by comparing the time constants of the swelling process. In the case of toxin-B-treated IMCD cells, the increase in P_f had to be calculated from the quotient τ $(A/V)_o$, because of the shape-changing effect of the toxin. P_f changes can be delineated quickly from two-dimensional scatter plots (τ values of untreated versus τ values of the same cells after treatment; Fig. 7).

In the case of primary cultured IMCD cells the osmotic water permeability was approximately doubled after two different stimuli (forskolin and toxin B). A similar increase was found in LLC-PK_1-cells stably transfected with AQP2 (Katsura et al., 1995). For other cell lines transfected with AQP2, e.g., CD8 cells (Valenti et al., 1996, 1998) or WT-10 cells (Deen et al., 1997), a three- to eightfold increase in osmotic water permeability after forskolin stimulation has been reported using various experimental approaches. The reason for these differences between various cell models is not clear, in particular because the P_f value of unstimulated IMCD cells (12.76 ± 3.43 μm/s) is in the same range as those reported for unstimulated CD8 cells and WT-10 cells.

The method presented here can be placed between the one-dimensional, fluorescent microbeads method and the three-dimensional variant (preloaded fluorophores). A two-dimensional parameter appears to be adequate because volume changes of adherent cells reveal basically only one degree of freedom during cell swelling or shrinkage, namely, that of cell height, with negligible lateral membrane displacement. Data reported by Korchev et al. (2000), comparing one- and three-dimensional approaches to measure osmotically induced cell volume kinetics, as well as our results indicate the validity of approaches omitting the calculation of total cell volume. LSRM is a method that leads to valid results without the requirement for pretreatment of cells with volume indicators and does not require additional hardware equipment. To our knowledge, this is the first report introducing reflection microscopy in combination with laser scanning microscopy in cell biology.

Considered together, the data presented here and those obtained by Klussmann et al. (2001) suggest that toxin B increases water permeability in primary cultured IMCD cells by translocation of AQP2-bearing vesicles from intracellular domains into the cell membrane in a cAMP-independent manner.

We thank Klaus Aktories (Freiburg, Germany) for providing *Clostridium difficile* toxin B, John Dickson for critically reading the manuscript, Andrea Geelhaar for superb technical assistance, Ricardo Hermosilla for help in statistical analysis, Brunhilde Oczko for technical assistance in manually analyzing the data sets of the first experimental recordings, Juergen Mevert for manufacturing customized cuvettes for the LSRM experiments, and Robert Storm for performing RT-PCR experiments.

This work was supported by a grant from the Deutsche Forschungsgemeinschaft (Ro 597/6–3) and by a grant from the Fonds der Chemischen Industrie.

REFERENCES

Burg, M., J. Grantham, M. Abranow, and J. Orloff. 1966. Preparation and study of fragments of single rabbit nephrons. *Am. J. Physiol.* 210: 1293–1298.

Crowe, W. E., and N. K. Wills. 1991. A simple method for monitoring changes in cell height using fluorescent microbeads and an Ussing-type chamber for the inverted microscope. *Pflügers Arch.* 419:349–357.

Deen, P. M. T., J. P. L. Rijss, S. M. Mulders, R. J. Errington, J. V. Baal, and C. H. van Os. 1997. Aquaporin-2 transfection of Madin-Darby canine kidney cells reconstitutes vasopressin-regulated transcellular osmotic water transport. *J. Am. Soc. Nephrol.* 8:1493–1501.

Farinas, J., V. Simanek, and A. S. Verkman. 1995. Cell volume measured by total internal reflection microflourimetry: application to water and solute transport in cells transfected with water channel homologues. *Biophys. J.* 68:1613–1620.

Filler, T. J., and E. T. Peuker. 2000. Reflection contrast microscopy (RCM): a forgotten technique? *J. Pathol.* 190:635–638.

Fisher, R. S., B. E. Persson, and K. R. Spring. 1981. Epithelial cell volume regulation: bicarbonate dependence. *Science.* 214:1357–1359.

Hall, A. 1998. Rho GTPases and the actin cytoskeleton. *Science.* 279: 509–514.

Katsura, T., J. M. Verbavatz, J. Farinas, T. Ma, D. A. Ausiello, A. S. Verkman, and D. Brown. 1995. Constitutive and regulated membrane expression of aquaporin 1 and aquaporin 2 water channels in stably transfected LLC-PK_1 epithelial cells. *Proc. Natl. Acad. Sci. U.S.A.* 92:7212–7216.

Klussmann, E., K. Maric, and W. Rosenthal. 2000. The mechanisms of aquaporin control in the renal collecting duct. *Rev. Physiol. Biochem. Pharmcol.* 141:33–95.

Klussmann, E., K. Maric, B. Wiesner, M. Beyermann, and W. Rosenthal. 1999. Protein kinase A anchoring proteins are required for vasopressin-mediated translocation of aquaporin-2 into cell membranes of renal principal cells. *J. Biol. Chem.* 274:4934–4938.

Klussmann, E., G. Tamma, D. Lorenz, B. Wiesner, K. Maric, F. Hofmann, K. Aktories, G. Valenti, and W. Rosenthal. 2001. An inhibitory role of Rho in the vasopressin-mediated translocation of aquaporin-2 into cell membranes of renal principal cells. *J. Biol. Chem.* 276: (in press).

Koeford-Johnson, V., and H. H. Ussing. 1953. The contributions of diffusion and flow to the passage of D_2O through living membranes. *Acta. Physiol. Scand.* 28:60–76.

Korchev, Y. E., J. Gorelik, M. J. Lab, E. V. Sviderskaja, C. L. Johnston, C. R. Coombes, I. Vodynoy, and C. R. W. Edwards. 2000. Cell volume measurement using scanning ion conductance microscopy. *Biophys. J.* 78:451–457.

Lerm, M., G. Schmidt, and K. Aktories. 2000. Bacterial protein toxins targeting Rho GTPases. *FEMS Microbiol. Lett.* 188:1–6.

Maric, K., A. Oksche, and W. Rosenthal. 1998. Aquaporin-2 expression in primary cultured rat inner medullary collecting duct cells. *Am. J. Physiol.* 275:F796–F801.

Mooren, F. C., and R. K. H. Kinne. 1994. Intracellular calcium in primary cultures of rat inner medullary collecting duct cells during variations of extracellular osmolality. *Pflügers Arch.* 427:463–472.

Preston, G. M., T. P. Carroll, W. B. Guggino, and P. Agre. 1992. Appearence of water channels in *Xenopus* oocytes expressing red cell CHIP28 protein. *Science*. 256:385–387.

Valenti, G., A. Frigeri, P. M. Ronco, C. D'Ettorre, and M. Svelto. 1996. Expression and functional analysis of water channels in a stably AQP2-transfected human collecting duct cell line. *J. Biol. Chem.* 271: 24365–24370. Correction: 1997, *J. Biol. Chem*. 272:26794.

Valenti, G., G. Procino, U. Liebenhoff, A. Frigeri, P. A. Benedetti, G. Ahnert-Hilger, B. Nürnberg, M. Svelto, and W. Rosenthal. 1998. A heterotrimeric G protein of the G_i family is required for cAMP-triggered trafficking of aquaporin 2 in kidney epithelial cells. *J. Biol. Chem.* 273:22627–22634.

Van Driessche, W., P. De Smet, and G. Raskin. 1993. An automatic monitoring system for epithelial cell height. *Pflugers Arch.* 425: 164–171.

Wade, J. B., D. L. Stetson, and S. A. Lewis. 1981. ADH action: evidence for membrane shuttle mechanism. *Ann. NY Acad. Sci.* 372:106–117.